Available online at www.sciencedirect.com
ScienceDirect
Developmental Biology 302 (2007) 80–91
DEVELOPMENTAL BIOLOGY
www.elsevier.com/locate/ydbio

FGF18 is required for early chondrocyte proliferation, hypertrophy and vascular invasion of the growth plate

Zhonghao Liu [1], Kory J. Lavine, Irene H. Hung, David M. Ornitz *

Department of Molecular Biology and Pharmacology, Washington University School of Medicine, 660 South Euclid Avenue, St. Louis, MO 63110, USA

Received for publication 9 June 2006; revised 29 August 2006; accepted 30 August 2006
Available online 5 September 2006

Abstract

Fibroblast growth factor 18 (FGF18) has been shown to regulate chondrocyte proliferation and differentiation by signaling through FGF receptor 3 (FGFR3) and to regulate osteogenesis by signaling through other FGFRs. *Fgf18*$^{-/-}$ mice have an apparent delay in skeletal mineralization that is not seen in *Fgfr3*$^{-/-}$ mice. However, this delay in mineralization could not be simply explained by FGF18 signaling to osteoblasts. Here we show that delayed mineralization in *Fgf18*$^{-/-}$ mice was closely associated with delayed initiation of chondrocyte hypertrophy, decreased proliferation at early stages of chondrogenesis, delayed skeletal vascularization and delayed osteoclast and osteoblast recruitment to the growth plate. We further show that FGF18 is necessary for *Vegf* expression in hypertrophic chondrocytes and the perichondrium and is sufficient to induce *Vegf* expression in skeletal explants. These findings support a model in which FGF18 regulates skeletal vascularization and subsequent recruitment of osteoblasts/osteoclasts through regulation of early stages of chondrogenesis and VEGF expression. FGF18 thus coordinates neovascularization of the growth plate with chondrocyte and osteoblast growth and differentiation.

Keywords: Fibroblast growth factor 18 (FGF18); Skeletal development; Growth plate; Chondrocyte; Osteoblast; Periosteum; Perichondrium; Vascular development

Introduction

Skeletogenesis in vertebrates is achieved through two distinct developmental processes. Cranial bones and medial clavicles are formed through intramembranous ossification, while facial bones and the appendicular skeleton develop through endochondral ossification (Erlebacher et al., 1995; Karsenty and Wagner, 2002). Shortly after limb bud formation, endochondral ossification is initiated from mesenchymal condensations. Differentiation of condensed mesenchyme gives rise to chondrocytes centrally and osteoprogenitors in the perichondrium. Proliferating chondrocytes and subsequently differentiated hypertrophic chondrocytes elaborate an extracellular matrix (ECM) that forms a cartilaginous template for future mineralization.

Fibroblast growth factors (FGFs) are signaling molecules that are essential regulators of endochondral bone growth. FGF receptor 3 (FGFR3) is expressed in proliferating chondrocytes where it regulates proliferation and differentiation. At late embryonic stages and during postnatal skeletal growth, FGFR3 signaling suppresses chondrocyte proliferation and hypertrophic differentiation (Goldring et al., 2006; Ornitz and Marie, 2002). However, during early skeletal development, FGFR3 is mitogenic for chondrocytes and inhibits hypertrophic differentiation (Iwata et al., 2000). FGF18 is expressed in the perichondrium and in joint spaces and has been identified as a potential ligand for FGFR3 (Davidson et al., 2005; Xu et al., 2000). At late embryonic stages, both *Fgf18*$^{-/-}$ and *Fgfr3*$^{-/-}$ mice have an expanded proliferating and hypertrophic chondrocyte zone, associated with increased Indian hedgehog (IHH) expression and signaling (Colvin et al., 1996; Liu et al., 2002; Naski et al., 1998; Ohbayashi et al., 2002). These similarities suggest that FGF18 is a functional ligand for FGFR3. However, *Fgf18*$^{-/-}$ mice have reduced bone length and show an approximate 2-day delay in the onset of skeletal mineralization, phenotypes that are not observed in *Fgfr3*$^{-/-}$ mice (Liu et al.,

* Corresponding author.
E-mail address: dornitz@wustl.edu (D.M. Ornitz).
[1] Current address: Department of Medicine, Washington University School of Medicine, USA.

0012-1606/$ - see front matter © 2006 Elsevier Inc. All rights reserved.
doi:10.1016/j.ydbio.2006.08.071

2002). This suggests that FGF18 signals to other FGFRs to regulate the onset of the mineralization process. The delayed mineralization phenotype in *Fgf18*$^{-/-}$ mice could be explained by either a direct effect of FGF18 on the chondrocyte and osteoblast or an indirect effect of FGF18 on, for example, vascularization of the growth plate.

The hypertrophic chondrocyte zone is an avascular structure that must be invaded by blood vessels that arise from the perichondrium. This neovasculogenesis of the central hypertrophic zone allows hematopoietic-derived osteoclasts/chondroclasts to enter and progressively erode the cartilaginous matrix (Goldring et al., 2006; Kronenberg, 2003; Wagner and Karsenty, 2001; Zelzer and Olsen, 2005). Along with the vasculature, perichondrial-derived osteoblasts eventually replace the eroded cartilaginous matrix with trabecular bone. Such a sequence of events relies on the precise coupling of chondrogenesis, osteogenesis and vascularization. However, it is still unclear how these different developmental processes are coordinated in a temporally and spatially correct fashion.

The endothelial cell-specific mitogen vascular endothelial growth factor (VEGFA) is an important regulator of vasculogenesis and angiogenesis during endochondral ossification. VEGFA binds to its tyrosine kinase receptors VEGFR1 (Flt1, VR1) and VEGFR2 (Flk1, VR2) (Yancopoulos et al., 2000). Administration of a soluble receptor to inhibit VEGF suppresses vascular invasion and results in bone length reduction and hypertrophic zone expansion (Gerber et al., 1999). Conditional targeting of VEGFA or VEGF164/188 in type II collagen-expressing cells and descendants produces similar phenotypes (Maes et al., 2002; Zelzer et al., 2002). These data demonstrate that VEGF/VEGFR signaling is essential for skeletal vascularization.

In this study, we demonstrate that the delayed ossification observed in *Fgf18*$^{-/-}$ mice was closely associated with delayed initiation of chondrocyte hypertrophy, skeletal vascularization and osteoclast recruitment, and decreased chondrocyte proliferation. We show that expression of *Vegf* in hypertrophic chondrocytes was also delayed in *Fgf18*$^{-/-}$ mice with concurrent decreased expression of *Vegfr1*. In an *in vitro* limb explant culture system, we demonstrated that FGF18 was sufficient to induce *Vegf* expression. These findings support a model in which FGF18 regulates skeletal vascularization and osteoclast recruitment through regulation of VEGF signaling. Combined with previous data, we conclude that FGF18 is an essential regulator of skeletogenesis by coordinating chondrocyte proliferation/differentiation, osteoblast proliferation and vascular invasion.

Materials and methods

Skeletal preparations

Skeletons were prepared as described previously (Liu et al., 2002). For postnatal day 0 (P0) skeletal preparations, carcasses were skinned and eviscerated, and then soaked in acetone for 12–24 h, cleared in 2% KOH (12–24 h), stained with alizarin red S and alcian blue (12–24 h), cleared in 1% KOH/20% glycerol, and stored in glycerol. For embryo skeleton preparations, fetuses were skinned and eviscerated, stained with alizarin red S and alcian blue (12–24 h), cleared in 1% KOH/20% glycerol, and stored in glycerol.

Histological and immunohistochemical analysis

Tissues were fixed in 4% paraformaldehyde/PBS, decalcified if necessary in EDTA or Decalcifying Solution (Stephens Scientific), and embedded in paraffin. Sections were stained with hematoxylin and eosin (H&E), von Kossa and TRAP. For PECAM (CD31) immunohistochemistry, sections were deparaffinized with two changes of xylene for 10 min each, then rehydrated through 100%, 95%, 75% and 50% ethanol washes for 5 min each. After rinsing in PBS, sections were treated with 0.1% trypsin at 37 °C for 10 min and rinsed in three changes of PBS for 5 min each. Sections were blocked in 5% serum for 30 min and then incubated with anti-PECAM antibody (BD Pharmingen) at 4 °C for 12–24 h, rinsed with PBS, and incubated with secondary antibody (Chemicon) at RT for 1 h. Fluorescent microscopic images were taken using a Hamumatsu camera and AxioVison3.0 software (Zeiss).

In situ hybridization

In situ hybridization was performed as described previously (Liu et al., 2002). The plasmids used for generating P^{33}-labeled riboprobes were generously provided by: B. Olsen (*Collagen X*, *Vegfr1*, *Vegfr2*); G. Karsenty (*Vegf*); G. Andersson (*Trap*); Z. Werb (*Mmp9*); A. McMahon (*Ihh*); H. Kronenberg (*Pth1r*); B. de Crombrugghe (*Sox9*, *Collagen 1*).

Real-time quantitative PCR

Total RNA was extracted from E16.5 skinned autopods using the RNeasy Mini kit (Qiagen, Valencia, CA). Two RNA samples from each genotype were pooled together, 1 μg of total RNA was used for oligo dT or random hexanucleotide-primed cDNA synthesis. cDNAs were added to 25 μl reaction mixtures containing 12.5 μl of SYBR Green master mix (Applied Biosystems, Foster City, CA), 0.25 U of UDP-N-glycosidase (Invitrogen), and 400 nM gene-specific primers. A melting curve was used to identify a temperature where only the amplicon, and not primer dimers, accounted for the SYBR green-bound fluorescence. Assays were performed in quadruplicate with an ABI Prism 7700 Sequence Detector (Applied Biosystems). All data were normalized to an internal standard (GAPDH; comparative C_T method, User Bulletin 2, Applied Biosystems).

Primer sequences:*Gapdh* (5′ TGCACCACCAACTGCTTAG 3′; 5′ GGATGCAGGGATGATGTTC 3′), *Flt1* (5′ GAGGAGGATGAGGGTGTCTATAGGT 3′; 5′ GTGATCAGCTCCAGGTTTGACTT 3′) (Shih et al., 2002), *Flk1* (5′ AGGTCACCATTCATCGCCTC 3′; 5′ GAAATCGACCCTCGGCATG 3′), *Pecam1* (5′ AGGAAAGCCAAGGCCAAACA 3′; 5′ CATTAAGGGAGCCTTCCGTTCT 3′) (Fitzsimmons et al., 2000), *VegfA* (5′ GGAGATCCTTCGAGGAGCACTT 3′; 5′ GGCGATTTAGCAGCAGATATAAGAA 3′) (Shih et al., 2002), *VegfB* (5′ GAAGAAAGTGGTGCCATGGATAG 3′; 5′ CCCATGAGTTCCATGCTCAGA 3′) (Mills et al., 2001).

PCR conditions for *Flt1* and *Flk1*: 50 °C 2 min; 95 °C 10 min; 35 (95 °C 15 s; 60 °C 1 min). PCR conditions for *VegfA, VegfB*: 95 °C 3 min; 40 (95 °C 30 s; 60 °C 30 s; 72 °C 30 s).

Embryonic limb explant cultures and whole mount β-galactosidase staining

Limb explant cultures were carried out essentially as described (Minina et al., 2001) with minor modifications. Forelimb cartilage was dissected from E14.5 VEGF-*LacZ* or wild type mouse embryos (Miquerol et al., 1999) and placed at the air-fluid interface on Transwell filters (Corning) containing DMEM, 10% fetal calf serum (GibcoBRL), antibiotic/antimycotic solution (Sigma) and 2 μg/ml heparin. Media was supplemented with 250 ng/ml recombinant FGF10 (Peprotech), recombinant FGF18 (Peprotech), or BSA. Explants were cultured for 24 h or 48 h at 37°C/5% CO_2 under humidified conditions. For whole mount β-galactosidase staining, limb explants were harvested on Day 2 and fixed in 0.2% glutaraldehyde, 5 mM EGTA pH 7.3, 100 mM $MgCl_2$, 0.02% NP40, 0.01% sodium deoxycholate in PBS. After washing with PBS, explants were incubated for 4–5 h at 24 °C in β-galactosidase staining buffer containing 1 mg/ml X-gal, 5 mM $K_3Fe(CN)_6$,

5 mM $K_4FE(CN)_63H_20$. Stained explants were rinsed in PBS prior to digital photography with an Olympus DP70 camera.

Results

Delayed ossification in Fgf18$^{-/-}$ mice

Examination of skeletal preparations from *Fgf18*$^{-/-}$ mice demonstrated delayed ossification in both intramembranous and endochondral skeletal elements. Cranial ossification begins around E14.5 in wild type mice. At E15.5, both the frontal and parietal bones of the cranium were clearly mineralized in wild type mice, as shown by Alizarin Red staining (Fig. 1A). In *Fgf18*$^{-/-}$ mice, Alizarin Red staining was absent in the cranium at this stage, while the maxilla, premaxilla and the mandible showed significant mineralization (Fig. 1A). However, the mandible was still underdeveloped in *Fgf18*$^{-/-}$ mice compared with that of wild type embryos (Fig. 1A). One day later at E16.5, mineralization of the *Fgf18*$^{-/-}$ cranium was not yet initiated (Fig. 1B). The developing ribs also showed delayed mineralization. At E16.5 in wild type embryos, the mineralized portion of the ribs extended almost halfway towards the ventral midline, but in *Fgf18*$^{-/-}$ mutants, ribs were deformed and only the dorsal most portions were mineralized (Fig. 1C). At E17.5, the rib deformity in *Fgf18*$^{-/-}$ mutants persisted and mineralization had progressed to a lesser degree compared to wild type littermates (Fig. 1D).

In addition to the ossification defects in the axial skeletons, the appendicular skeleton also showed delayed ossification (Liu et al., 2002). At E17.5, the mineralized portions of the limbs in *Fgf18*$^{-/-}$ embryos were significantly shorter than those of wild type littermates (Fig. 1E). Additionally, ossification centers in the metacarpal bones were present in wild type mice, but were not initiated in *Fgf18*$^{-/-}$ embryos at this stage (Fig. 1E). Similar

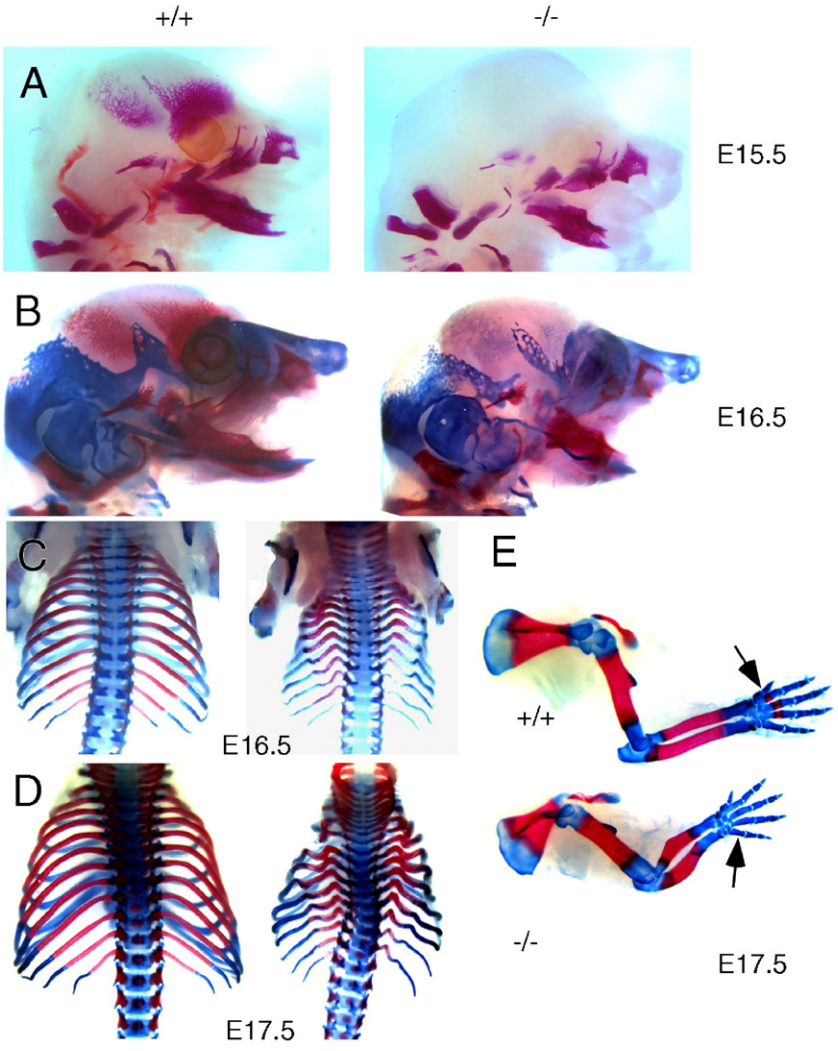

Fig. 1. Morphological analysis of skeletal ossification. (A) Alizarin red-stained skull from an E15.5 wild type littermate (left) and an *Fgf18*$^{-/-}$ embryo (right) showing delayed ossification in the *Fgf18*$^{-/-}$ mutant. (B) Alizarin red- and alcian blue-stained skull from an E16.5 wild type littermate (left) and an *Fgf18*$^{-/-}$ embryo (right). Note the delayed ossification in the cranium of the *Fgf18*$^{-/-}$ mutant. (C) Alizarin red- and alcian blue-stained ribs from an E16.5 wild type littermate (left) and an *Fgf18*$^{-/-}$ embryo (right). Note the deformed ribs and poorly ossified ribs of the *Fgf18*$^{-/-}$ embryo. (D) Alizarin red- and alcian blue-stained ribs from an E17.5 wild type littermate (left) and an *Fgf18*$^{-/-}$ embryo (right). (E) Forelimbs from an E17.5 wild type littermate (upper) and an *Fgf18*$^{-/-}$ embryo (lower). Note there is no ossification of the autopod elements of the *Fgf18*$^{-/-}$ embryo at this stage (arrow).

defects were also observed in phalangeal bones at later stages of development and in the zeugopod and stylopod at earlier stages of development (Liu et al., 2002, and data not shown). These data demonstrated that the onset of ossification in *Fgf18*$^{-/-}$ mice was delayed in skeletal elements involving both endochondral and intramembranous ossification.

In endochondral bone growth, the progression of chondrocyte development results in mineralization of the cartilaginous matrix of the completely differentiated hypertrophic chondrocyte (Karsenty and Wagner, 2002). Cartilage matrix mineralization is thought to be essential for subsequent vascular invasion and ossification. Because of the observed delay in skeletal ossification, it was important to determine whether there was also a delay in mineralization of hypertrophic chondrocytes and formation of the bone collar. Von Kossa staining of skeletal elements was used to examine the extent of ossification. In the autopods, mineralization of the metatarsal elements in wild type embryos was seen in the middle of the cartilage element at E16.5 (Fig. 2A). In *Fgf18*$^{-/-}$ metatarsals, no von Kossa staining was observed even though hypertrophic chondrocytes were present centrally (Fig. 2B). Furthermore, the perichondrium was thinner in *Fgf18*$^{-/-}$ metatarsals, suggesting a defect in bone collar formation. We next examined the expression of the bone-specific marker *Col1* to measure the extent of the defect. At E16.5, wild type metatarsal elements showed strong and localized *Col1* expression in the perichondrium adjacent to the hypertrophic chondrocytes (Fig. 2C), indicating the presence of osteoblasts. However, in *Fgf18*$^{-/-}$ metatarsals, only low-level expression of *Col1* was detected (Fig. 2D). One day later at E17.5, mineralization was initiated in *Fgf18*$^{-/-}$ metatarsals (Fig. 2F), but the extent of mineralization was significantly less than that of wild type littermates (Fig. 2E). Examination of the perichondrium showed significant mineralization in wild type metatarsal elements (Figs. 2E, G). However, at E17.5, *Fgf18*$^{-/-}$ metatarsal elements still showed minimal perichondrial/periosteal mineralization (Figs. 2F, H). Only a single layer of cuboidal osteoblasts was present in the perichondrium of *Fgf18*$^{-/-}$ metatarsal elements compared to several layers in wild type controls (Figs. 2G, H). This histology is consistent with less bone collar formation as shown by *Col1* expression (Figs. 2C, D). These data demonstrate that in *Fgf18*$^{-/-}$ mice, both perichondrial/periosteal bone collar formation and hypertrophic chondrocyte mineralization were delayed.

Delayed initiation of chondrocyte hypertrophy in Fgf18$^{-/-}$ *mice*

The observed delayed mineralization of hypertrophic chondrocytes suggested a more general delay in chondrocyte differentiation. Consistent with this, the hypertrophic chondrocyte portion of the skeletal elements in the autopods shown in Fig. 2 appeared to be significantly narrower in *Fgf18*$^{-/-}$ mice compared to wild type littermates, suggesting a possible delay in the initiation of chondrocyte hypertrophy (Figs. 2A–F). To confirm this, the extent of chondrocyte hypertrophy was evaluated by examining the expression of the hypertrophic chondrocyte-specific marker, type X collagen (*ColX*). At E15.5, the developing metatarsals showed a narrower domain of *ColX* expression in *Fgf18*$^{-/-}$ autopods compared to those of wild type littermates (Figs. 2I, J), consistent with the histology and delayed appearance of von Kossa-positive cells in the *Fgf18*$^{-/-}$ autopods.

We next examined proximal long bones to see if this delayed initiation of chondrocyte hypertrophy also existed in other skeletal elements. Histological analysis showed that the size of the hypertrophic chondrocyte zone in E14.5 *Fgf18*$^{-/-}$ humeri was significantly shorter than that in wild type littermates (0.53 mm versus 0.69 mm, respectively; $n=2$ mice for each genotype, 6 sections, $P<0.05$) (Figs. 3A, B). Similar delayed initiation of chondrocyte hypertrophy was also observed in other long bones (data not shown). These data demonstrate that FGF18 positively regulates the initiation of chondrocyte hypertrophy during early chondrogenesis and is likely to function in both proximal and distal skeletal elements.

To further characterize the nature of the chondrocyte phenotypes, we examined the expressions of several molecules that are important for the development of early chondrocytes. *In situ* hybridization experiments showed similar levels of expression of *Sox9* and the *PTHrP receptor* (*Pth1r*) in the growth plates of both *Fgf18*$^{-/-}$ and wild type mice (Figs. 3C–F). However, the expression of *Indian hedgehog* (*Ihh*), an important signaling molecule that controls the proliferation of chondrocytes, was decreased in the early hypertrophic chondrocytes of the E14.5 humerus from *Fgf18*$^{-/-}$ mice compared to that of wild type littermates (Figs. 3G, H). Similar down-regulation of *Ihh* was also observed in the tibia of *Fgf18*$^{-/-}$ mice (data not shown).

Decreased chondrocyte proliferation in E14.5 Fgf18$^{-/-}$ *mice*

Proliferation and differentiation of chondrocytes in the epiphyseal growth plate must be coordinated to keep long bone growth in balance. The delayed ossification and initiation of chondrocyte hypertrophy in *Fgf18*$^{-/-}$ mice could be due to a decreased pool of available proliferating chondrocytes. This possibility suggests that FGF18 could positively regulate chondrocyte proliferation during early chondrogenesis. To test this hypothesis, we assessed the proliferation rates of reserve and proliferating chondrocytes in E14.5 *Fgf18*$^{-/-}$ embryos. Proliferating cells were identified by immunohistochemical staining of phospho-histone 3 (pH3) (Fig. 4). pH3-positive cells in the proliferating zones of the distal tibia and humeri were decreased by 26% ($P<0.05$) and 31% ($P<0.05$), respectively (Figs. 4A–B and Table 1). However, chondrocytes in the reserve zones of these growth plates did not show statistically significant changes in the rate of proliferation (Table 1). Chondrocytes in the developing E14.5 metatarsals also showed markedly decreased rates of proliferation (Figs. 4C, D and Table 1). These data suggest that FGF18 promotes chondrocyte proliferation during early chondrogenesis, and are consistent with the observation of decreased *Ihh* expression in the growth plates of E14.5 *Fgf18*$^{-/-}$ mice (Figs. 3G, H). Cell death was assayed by TUNEL labeling. Very few apoptotic cells were observed at this stage of development and there was

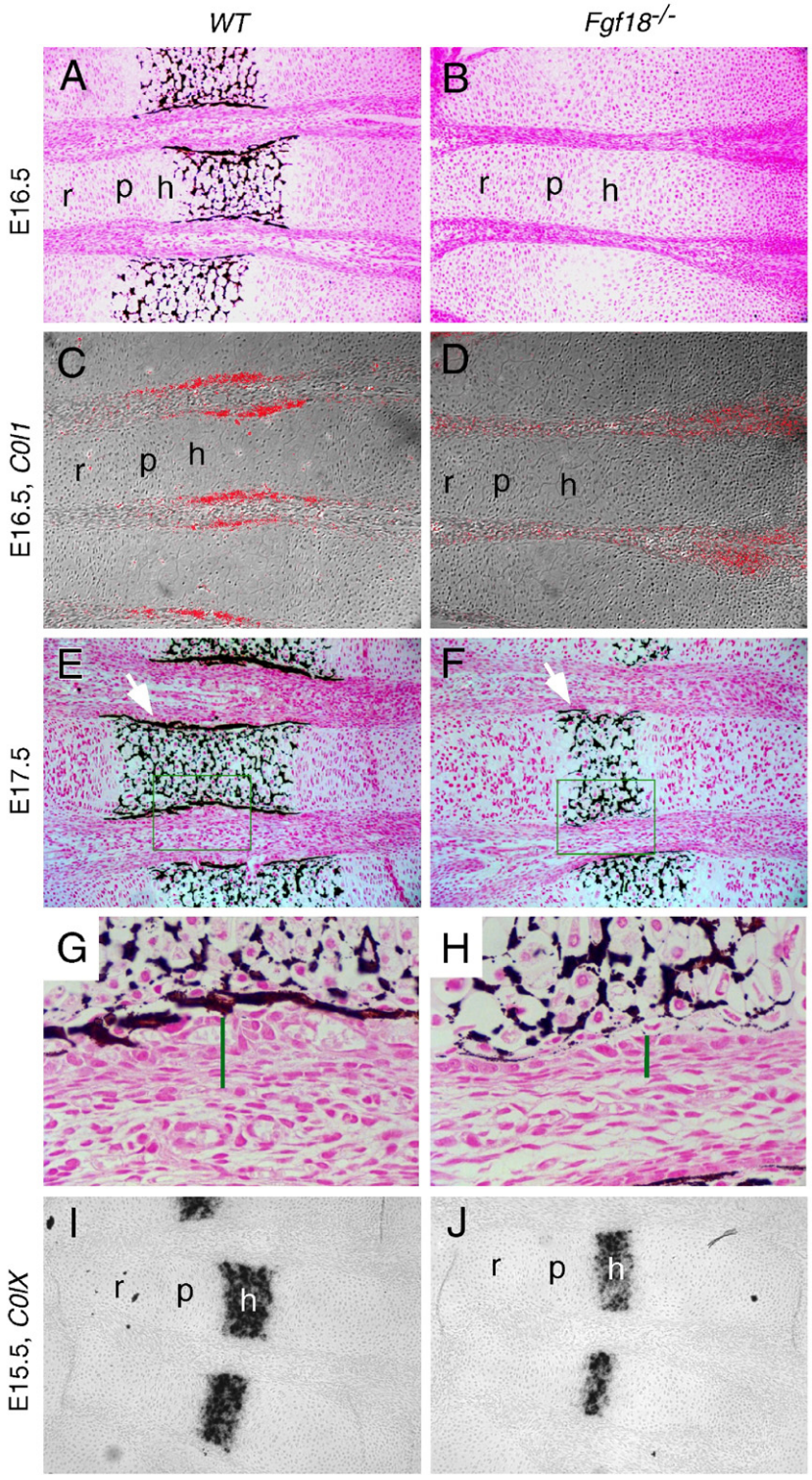

Fig. 2. Analysis of mineralization and initiation of chondrocyte hypertrophy in the developing autopod. (A, B, E–H) Von Kossa-stained sections to visualize mineralized tissue. (A, B) Metatarsal bones from an E16.5 wild type (A) and *Fgf18*$^{-/-}$ (B) embryo. Note there is no mineralization in *Fgf18*$^{-/-}$ metatarsals and fewer hypertrophic appearing cells. (C, D) *In situ* detection of *Col1* mRNA on sections of metatarsal bones from an E16.5 wild type (C) and *Fgf18*$^{-/-}$ (D) embryo. (E, F) Metatarsal bones from an E17.5 wild type (E) and *Fgf18*$^{-/-}$ (F) embryo. Note decreased mineralization of hypertrophic chondrocytes and less periosteal mineralization (arrows) in *Fgf18*$^{-/-}$ metatarsals. (G, H) High power view of the boxed area in panels E and F showing a thinner periosteum (green line) and an unmineralized bone collar in *Fgf18*$^{-/-}$ mice. (I, J) *In situ* detection of *ColX* on sections of metatarsal bones from an E15.5 wild type (I) and *Fgf18*$^{-/-}$ embryo (J) showing a narrower hypertrophic zone in the *Fgf18*$^{-/-}$ tissue. r, reserve chondrocytes; p, proliferating chondrocytes; h, hypertrophic chondrocytes. Panels A–H, I, J were photographed through a 10× objective. Panels G, H were photographed through a 20× objective and digitally magnified.

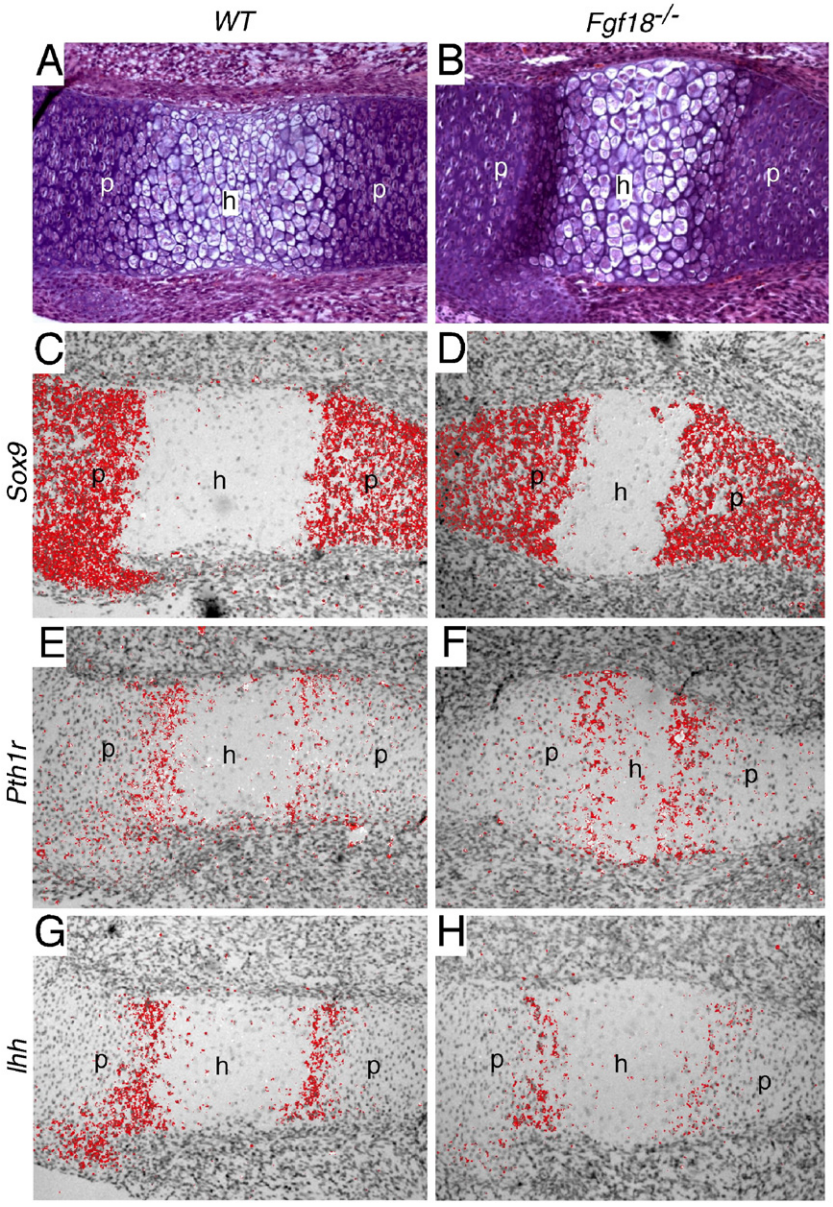

Fig. 3. Analysis of the initiation of chondrocyte hypertrophy in E14.5 wild type and *Fgf18*$^{-/-}$ mice. (A, B) Hematoxylin and eosin-stained sections of the humerus from an E14.5 wild type embryo (A) and an *Fgf18*$^{-/-}$ (B) embryo. Note the decreased length of the *Fgf18*$^{-/-}$ hypertrophic zone relative to that of the control. (C–H) *In situ* detection of *Sox9* (C, D), *PTHrP receptor* (*Pth1r)* (E, F) and *Indian Hedgehog* (*Ihh*) (G, H) in the developing humeri growth plates from E14.5 wild type embryos (C, E, G) and *Fgf18*$^{-/-}$ embryos (D, F, H). All panels were photographed through a 10× objective.

no apparent difference between control and *Fgf18*$^{-/-}$ mice (data not shown).

Delayed osteoclast recruitment into the hypertrophic chondrocyte zone in Fgf18$^{-/-}$ *mice*

Our data indicate that the decreased chondrocyte proliferation/hypertrophy and mineralization may be one mechanism resulting in delayed ossification in *Fgf18*$^{-/-}$ mice. However, definitive ossification requires vascular invasion of the avascular cartilaginous template allowing osteoblasts and osteoclasts to enter the central hypertrophic chondrocyte region. Previous studies on *Fgf18*$^{-/-}$ mice proposed that the delay in osteoblast colonization of the central hypertrophic zone resulted from either a direct effect of FGF18 on osteoblast proliferation or an effect on vascular invasion of the growth plate (Liu et al., 2002). Because both osteoblasts and osteoclasts require vasculature to gain entry into the hypertrophic zone (Karsenty and Wagner, 2002; Vu et al., 1998), we could test whether delayed vascular invasion could contribute to the observed phenotype by examining whether osteoclast recruitment was also delayed in the *Fgf18*$^{-/-}$ skeletons.

Osteoclasts/chondroclasts express tartrate-resistant acid phosphatase (TRAP) and matrix metalloproteinase 9 (MMP9) (Karsenty, 2003; Roodman, 1996; Vu et al., 1998). The expression of *Mmp9* is required for normal degradation of the cartilaginous matrix and vascularization of the hypertrophic zone. Consistent with this, *Mmp9*$^{-/-}$ mice have decreased angiogenesis and an

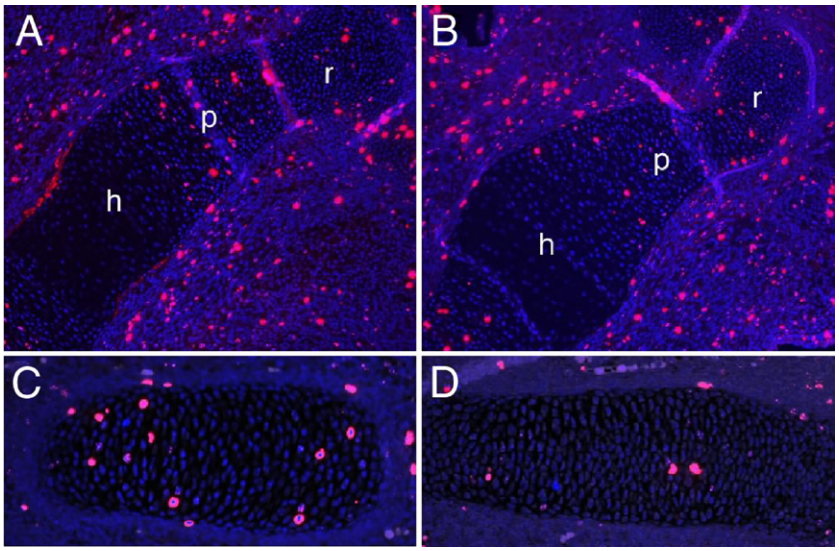

Fig. 4. Decreased chondrocyte proliferation in the growth plates of E14.5 mice. (A–D) proliferating cells were identified by immunostaining with a pH3 antibody (red), nuclei were stained with DAPI (blue). (A, B) pH3 staining of E14.5 distal humeri growth plates from a wild type (A) and an *Fgf18*$^{-/-}$ (B) embryo. (C, D) pH3 staining of E14.5 metatarsals from a wild type embryo (C) and an *Fgf18*$^{-/-}$ (D) embryo. r, reserve chondrocytes; p, proliferating chondrocytes; h, hypertrophic chondrocytes. All panels were photographed through a 10× objective.

expanded hypertrophic chondrocyte zone (Vu et al., 1998). At E15.5, when vascularization is initiated in the femur of wild type mice, both *Trap* and *Mmp9* transcripts can readily be detected in the vascular invasion front (Figs. 5A, C). However, expressions of *Trap* and *Mmp9* were significantly decreased in the femur of *Fgf18*$^{-/-}$ mice (Figs. 5B, D). By E16.5, in the developing humerus, endothelial cells have already populated the trabecular region and *Trap*-positive cells mostly reside at the cartilage-bone interface. In *Fgf18*$^{-/-}$ mice, there were fewer *Trap*-expressing cells in this region (17.5±2.6 in wild type versus 12±2.2 in *Fgf18*$^{-/-}$, $P<0.01$ and Figs. 5E, F). These data demonstrate that osteoclast infiltration into the hypertrophic zone was delayed in *Fgf18*$^{-/-}$ mice.

Reduced expression of Vegf and Vegf receptors in Fgf18$^{-/-}$ *mice*

Vascular endothelial growth factor (VEGF) signaling is essential for skeletal vascularization (Maes et al., 2002; Ornitz, 2005; Zelzer et al., 2002; Zelzer and Olsen, 2005). The delayed ossification and osteoclast recruitment in *Fgf18*$^{-/-}$ mice suggested that FGF18 might regulate skeletal vascularization through VEGF signaling. To test this hypothesis, we examined the expression of *Vegf* and *Vegf receptors* (*Vegfrs*) in developing skeletal elements. In wild type E15.5 autopods, *Vegf* expression was present in hypertrophic chondrocytes and in interdigital mesenchyme (Figs. 6A, A′). In *Fgf18*$^{-/-}$ autopods, the expression of *Vegf* was reduced, especially in the hypertrophic chondrocyte region (Figs. 6B, B′). Consistent with this, quantitative real-time PCR analysis of E16.5 autopods showed a 37% decrease in *VegfA* expression (Fig. 6G). However, in proximal long bones where chondrocytes have already undergone hypertrophy, the expression level of *VegfA* in *Fgf18*$^{-/-}$ mice appeared relatively normal (Liu et al., 2002). These data suggest that FGF18 may regulate *Vegf* expression in hypertrophic chondrocytes and the perichondrium at early stages of chondrocyte development.

The expression of *Vegfrs* is regulated by VEGF signaling, and the level of *Vegfr* expression serves as a measure of the strength of the VEGF signal (Barleon et al., 1997; Gerber et al., 1999; Shen et al., 1998; Zelzer et al., 2002). To test whether loss of FGF18 affects VEGF signaling, we compared the expression of *Vegfr1* and *Vegfr2* in wild type and *Fgf18*$^{-/-}$ mice. At E14.5 in the autopods, expressions of both *Vegfr1* and *Vegfr2* were detected in interdigital mesenchyme surrounding the metacarpal cartilage in wild type mice (Figs. 6C, E). In *Fgf18*$^{-/-}$ mice, the intensity of the *Vegfr1* and *Vegfr2* signals was weaker compared to wild type littermates (Figs. 6D, F). The expression of *Vegfr1* and *Vegfr2* was quantified using real-time PCR. At E16.5, both *Vegfr1* and *Vegfr2* were down-regulated, consistent with the ISH data. Interestingly, the extent of *Vegfr1* down-regulation (77% of wild type levels) was greater than *Vegfr2* (46% of wild type levels) (Fig. 6G). These data suggest that FGF18 may differentially affect *Vegfr1* and *Vegfr2* expression.

Table 1
Proliferation index for E14.5 growth plates

Growth plate [a]	Genotype	*N* [b]	pH3+/mm^2 [c]	Control (%)	*P* value
Distal tibia PZ	+/+	4	56.5±5.4	74	0.03
	−/−	4	42±8.3		
Distal tibia RZ	+/+	4	61.6±15.1	89	0.23
	−/−	4	54.8±5.8		
Distal humerus PZ	+/+	6	45.5±17.5	69	0.03
	−/−	8	31.4±8.3		
Distal humerus RZ	+/+	6	55.3±15.1	78	0.06
	−/−	8	43.1±12.4		
Metatarsal	+/+	5	58.5±9.9	63	0.002
	−/−	6	37±8.6		

[a] PZ, proliferating chondrocyte zone; RZ, reserve chondrocyte zone.
[b] Number of sections derived from at least 2 pairs of animals.
[c] pH3-positive cells per mm^2.

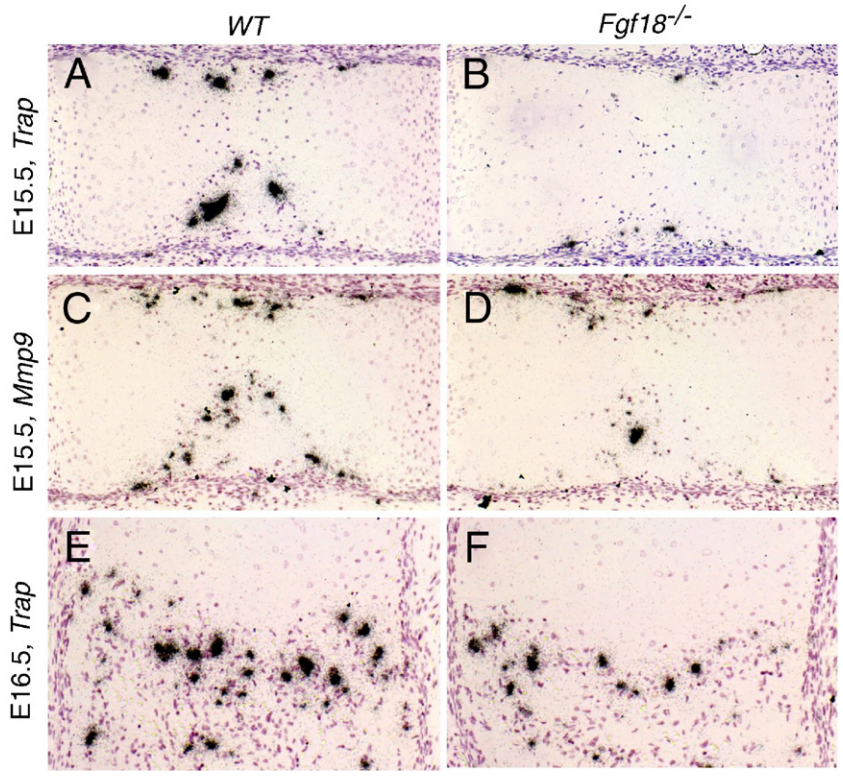

Fig. 5. Delayed osteoclast recruitment in *Fgf18*$^{-/-}$ mice. (A–D) *In situ* detection of *Trap* (A, B) and *Mmp9* (C, D) in the developing E15.5 femur. Note that fewer osteoclasts are present in the vascular front of the *Fgf18*$^{-/-}$ (B, D) compared to control (A, C) femora. (E, F) *In situ* detection of *Trap* in the developing E16.5 humerus from a wild type (E) and *Fgf18*$^{-/-}$ (F) mouse, showing fewer *Trap*-positive cells at the bone–cartilage interface of the *Fgf18*$^{-/-}$ humerus. All panels were photographed through a 10× objective.

To test whether reduced VEGF signaling in *Fgf18*$^{-/-}$ growth plate results in decreased vascularization, we examined vascular formation in E14.5 forelimbs. At this stage of development, *Fgf18* is expressed in the perichondrium, as shown by immunostaining for the β-galactosidase gene introduced into the *Fgf18* locus (Liu et al., 2002) (Figs. 7A, B). The pattern of β-galactosidase expression indicates sites where *Fgf18* is normally expressed. As visualized by PECAM immunohistochemistry, blood vessels were present in close proximity to developing hypertrophic chondrocytes in the humerus of wild type mice (Fig. 7A). However, the density of PECAM-expressing endothelial cells was significantly decreased in age-matched *Fgf18*$^{-/-}$ mice (Fig. 7B). These data demonstrate that FGF18 is required for VEGF expression and subsequent vascularization in the perichondrium.

FGF18 induces Vegf-LacZ expression in limb explant cultures

To test whether FGF18 could affect VEGF signaling more directly, we used a limb explant culture system. E14.5 forelimbs from mice heterozygous for a β-galactosidase-tagged allele of *Vegf* (Miquerol et al., 1999) were cultured with bovine serum albumin (BSA), FGF10, or FGF18. *Vegf* expression levels, as indicated by β-galactosidase staining intensity, were significantly increased in limbs treated with FGF18 compared with those treated with BSA or FGF10 (Figs. 7C–H). Furthermore, only FGF18-treated explants showed β-galactosidase activity in the perichondrium (Fig. 7H). Real-time quantitative PCR analysis was used to directly measure *Vegf* expression in wild type explants treated with BSA, FGF10, or FGF18. This analysis showed that *VegfA* expression was increased approximately 29% ($P=0.055$) after 24 h of FGF18 treatment (Fig. 7I). Though not statistically significant ($P=0.14$), *VegfB* may be upregulated as well. FGF10 did not induce expression of either *VegfA* or *VegfB* when compared to treatment with BSA (Fig. 7I). These results demonstrate that FGF18 is sufficient to induce *Vegf* expression in the limb. Furthermore, since FGF18 was active and FGF10 showed no activity, it indicated that a mesenchymal FGFR responded to the FGF18 signal. Since VEGF is an important stimulator of skeletal angiogenesis (Zelzer et al., 2002), these data support the hypothesis that FGF18 regulates vascularization of developing bone by positively regulating VEGF expression and signaling.

Discussion

In this study, we have extended the analysis of FGF18 function in skeletal development to show that at early embryonic stages (E14–E15), FGF18 signaling regulates chondrocyte proliferation, the onset of hypertrophic chondrocyte differentiation, vascular development in mesenchyme surrounding developing skeletal elements, and vascular invasion of the hypertrophic chondrocyte zone. These studies support a model in which FGF18 signals to FGFR3 in

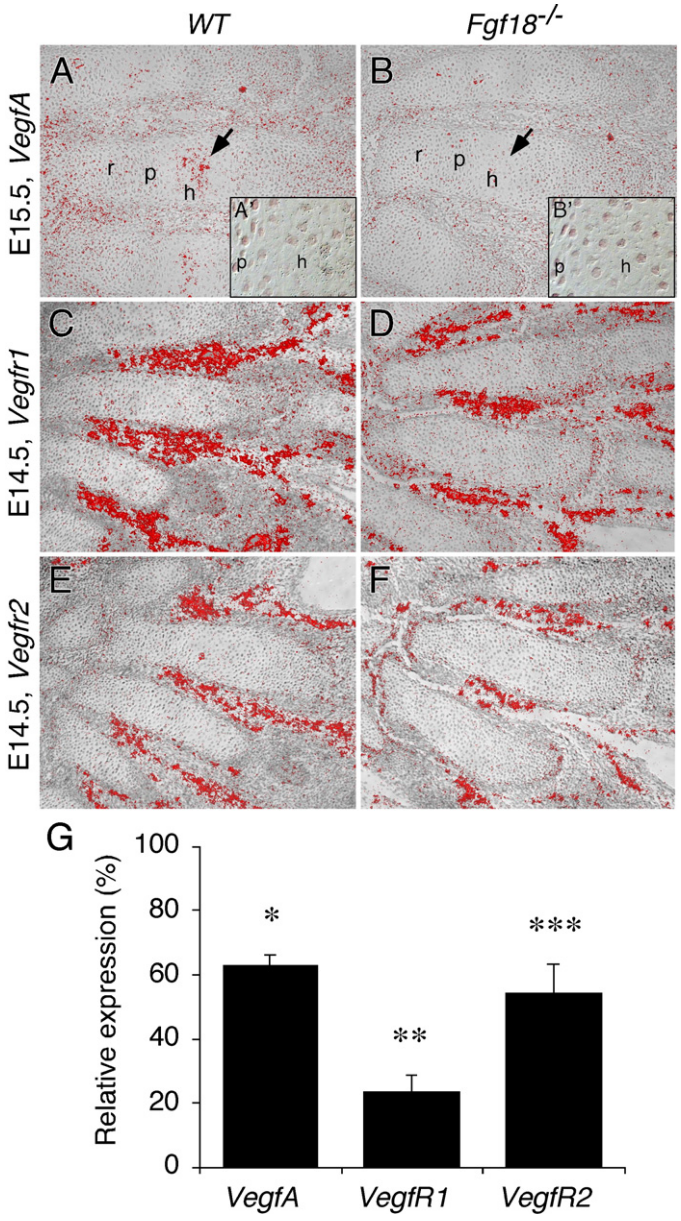

Fig. 6. Expression of *Vegf* and *Vegf receptors* in the developing autopod. (A, B) *In situ* detection of *VegfA* in the developing E15.5 autopod from a wild type (A) and *Fgf18*$^{-/-}$ (B) mouse. Arrow indicates *VegfA* expression in hypertrophic chondrocytes. r, reserve chondrocytes; p, proliferating chondrocytes; h, hypertrophic chondrocytes. (A′, B′) insets showing high magnification (40× objective) DIC images of the proliferating–hypertrophic chondrocyte junction of the darkfield overlays shown in panels A and B. Note that silver grains are visible in wild type hypertrophic chondrocytes in panel A′. (C, D) *In situ* detection of *Vegfr1* in the developing E14.5 autopod from a wild type (C) and *Fgf18*$^{-/-}$ (D) mouse. (E, F) *In situ* detection of *Vegfr2* in the developing E14.5 autopod from a wild type (E) and *Fgf18*$^{-/-}$ (F) mouse. Note that the *Vegfr1* and *Vegfr2* expression domains in the *Fgf18*$^{-/-}$ autopod are restricted to the middle region of the interdigital mesenchyme. Panels A–F were photographed through a 10× objective. (G) Real-time quantitative PCR analysis of *VegfA*, *Vegfr1* and *Vegfr2* expression. Data are expressed as the percentage of each individual gene's expression level (±SEM) in *Fgf18*$^{-/-}$ autopod tissue normalized to *Gapdh* expression, relative to the gene's expression level in wild type tissue normalized to *Gapdh* expression. (**P*<0.0001; ***P*=0.001; ****P*=0.005).

chondrocytes, and to other FGFRs in the perichondrium, to carry out its developmental and physiological role.

Regulation of chondrocyte proliferation and hypertrophy at early and late developmental stages

Skeletal development is unique in that it begins in midgestation and continues postnatally until puberty. Gain of function mutations in FGFR3 in humans and mice result in skeletal dwarfism by negatively regulating chondrocyte proliferation. The dwarfism phenotype is manifest during late embryogenesis and throughout the postnatal skeletal growth period. During this period of development, FGFR3 has been shown to negatively regulate chondrocyte proliferation and hypertrophic differentiation by activating STAT1 signaling pathways (Sahni et al., 1999, 2001). However, *in vitro*,

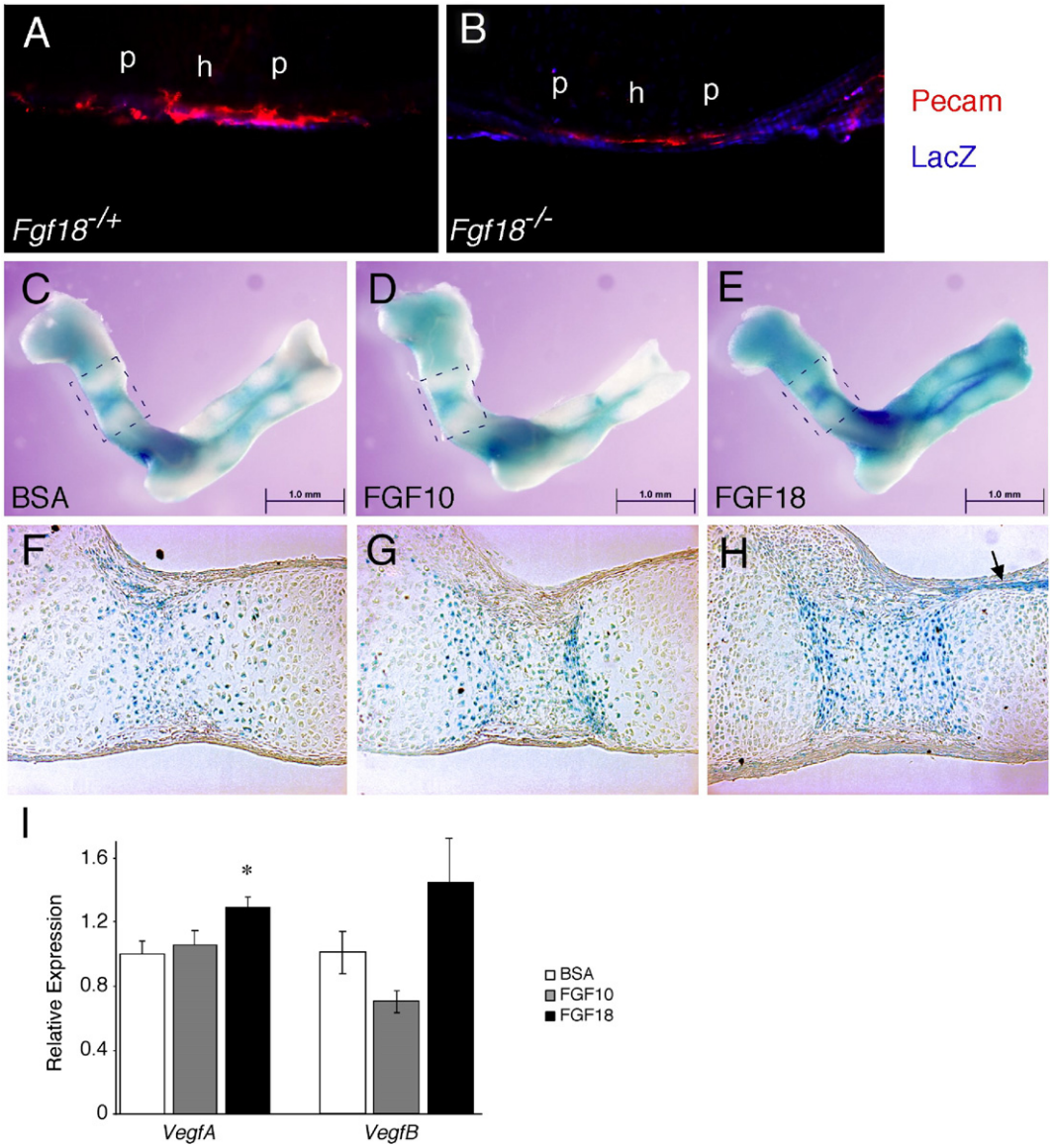

Fig. 7. FGF18 regulates *Vegf* expression in limb explant cultures. (A, B) Fluorescent immunohistochemical detection of perichondrial vasculature in the humeri of an E14.5 *Fgf18*$^{-/+}$ (A) and *Fgf18*$^{-/-}$ (B) mouse. Vascular endothelial cells were detected by immunostaining with a PECAM antibody (red). FGF18-expressing cells were detected by immunostaining with an antibody to β-galactosidase (blue). p, proliferating chondrocytes; h, hypertrophic chondrocytes. (C–H) Heterozygous *Vegf-LacZ* mouse forelimbs were explanted at E14.5 and cultured in the presence of BSA (C, F), FGF10 (D, G) or FGF18 (E, H) for 48 h. (F–H) Sections of boxed area in panels C–E showing β-galactosidase enzyme activity in hypertrophic chondrocytes. Note that FGF18-treated explant showed increased β-galactosidase activity, indicating that specific activation of mesenchymal FGF receptors can induce *Vegf* expression (E, H). Arrow points to β-galactosidase activity in the perichondrium of FGF18-treated explants (H). (I) Real-time quantitative RT-PCR analysis of *VegfA* and *VegfB* expression in wild type explants treated with BSA, FGF10 or FGF18. Data are expressed as the percentage of each individual gene's expression level in FGF10- or FGF18-treated samples, relative to the gene's expression level in BSA-treated samples (±SEM). All data were normalized to *Gapdh* expression before comparison. (*P=0.055).

activating mutations in FGFR3 are mitogenic (Naski et al., 1996). Examination of mice harboring an activating mutation in FGFR3 revealed that early in development, FGFR3 functions to promote chondrocyte proliferation and decrease differentiation (Iwata et al., 2000). This suggests that signaling through FGFR3 has a biphasic role during chondrocyte development: first, promoting chondrocyte proliferation at early embryonic stages; and later, acting to suppress chondrocyte proliferation. Consistent with this model, cultured limb mesenchymal cells from *Fgfr3*$^{-/-}$ mice fail to differentiate into chondrocytes and do not proliferate in the presence of FGF18 (Davidson et al., 2005).

In the initial analysis of *Fgf18*$^{-/-}$ mice, it was noted that at late developmental stages, the hypertrophic chondrocyte zone was expanded, with histology similar to that seen in mice lacking *Fgfr3*. This was consistent with a model in which FGF18 signaled through FGFR3 to negatively regulate chondrocyte proliferation and differentiation during late embryonic and early postnatal development. In this study, we examined the *Fgf18*$^{-/-}$ phenotype at early embryonic stages and found that the size of the early hypertrophic chondrocyte zone was significantly decreased at E14.5, suggesting decreased chondrocyte proliferation and a delay in the initiation

of chondrocyte hypertrophy. Indeed, quantification of proliferating cells showed significantly decreased chondrocyte proliferation in E14.5 *Fgf18*$^{-/-}$ growth plates. This paradoxical effect on chondrocyte proliferation and differentiation supports a model in which chondrocytes at different stages of development may switch their cellular responsiveness to FGF18/FGFR3 signaling from a mitogenic/differentiation response to a non-mitogenic/reduced differentiation response. Alternatively, the shortened hypertrophic chondrocyte zone could be explained by a more general delay in endochondral bone development.

Previous studies showed that FGF18 and FGFR3 inhibited *Ihh* expression in pre-hypertrophic chondrocytes at late embryonic and postnatal stages (Liu et al., 2002; Naski et al., 1998). The primary role of IHH is to regulate chondrocyte maturation through induction of PTHrP (St-Jacques et al., 1999). During early chondrogenesis, IHH also stimulates chondrocyte proliferation in a largely *PTHrP*-independent pathway (Karp et al., 2000). Our observation of the concomitant decreases in both *Ihh* expression and chondrocyte proliferation suggests that FGF18/FGFR3 may regulate chondrocyte proliferation and differentiation indirectly by regulating IHH signaling. In support of this model, Iwata et al. observed increased chondrocyte proliferation and increased *Patched* expression in E15.5 mice harboring an *Fgfr3* gain of function mutation (Iwata et al., 2000).

Delayed vascularization and osteoclast recruitment

Endochondral bone growth is a complex process that involves three different but related developmental events: chondrogenesis, vascularization and osteogenesis (Karsenty and Wagner, 2002; Kronenberg, 2003; Ornitz, 2005; Ornitz and Marie, 2002). Vascularization is essential to transform cartilage matrix into trabecular bone by facilitating the influx of both osteoblasts and osteoclasts. The observations that in *Fgf18*$^{-/-}$ mice, osteoblast (Liu et al., 2002) and osteoclast markers (Fig. 5) are down-regulated in the trabecular region of developing long bones, indicate that the influx of both osteoblasts and osteoclasts is delayed in the absence of FGF18 signaling. The delayed entry of the hematopoietic-derived osteoclast suggests that a primary mechanism accounting for the delayed formation of the ossification center in *Fgf18*$^{-/-}$ mice is a delay in vascularization of the growth plate. Furthermore, since this delay is not seen in *Fgfr3*$^{-/-}$ mice, it is likely that delayed vascularization is mediated through FGFR1 and/or FGFR2 signaling in perichondrial tissue or FGFR1 signaling in hypertrophic chondrocytes.

In addition to delayed vascularization, it is also possible that maturation of the osteoclast is itself delayed. Osteoclasts express *Fgfr1* and could respond directly to FGF18; alternatively, osteoclast maturation could be affected indirectly by altered FGF-mediated cytokine production by osteoblasts (Chikazu et al., 2000; Chikazu et al., 2001). However, the decreased number of osteoclasts at the vascular front suggests that delayed vascularization is the predominant factor delaying skeletal vascularization in *Fgf18*$^{-/-}$ mice.

VEGF and FGF signaling are two major pathways that regulate vasculogenesis and angiogenesis (Cross and Claesson-Welsh, 2001; Yancopoulos et al., 2000). VEGF signaling is essential for the vascularization of developing cartilage (Carlevaro et al., 2000; Gerber et al., 1999; Haigh et al., 2000; Zelzer et al., 2002). The delayed skeletal vascularization in *Fgf18*$^{-/-}$ mice could result from decreased FGF signaling directly to endothelial cells or indirectly through regulation of VEGF signaling. Embryos in which both *Fgfr1* and *Fgfr2* have been conditionally inactivated in endothelial cells develop normally and are viable (Lavine et al., 2006). These mice do not exhibit defects in skeletal vascularization (KJL and DMO, unpublished observation), suggesting that FGF18 may regulate vascular growth indirectly by regulating *Vegf* expression. Consistent with this model, we showed that in the absence of FGF18, *Vegf* expression is decreased/delayed in hypertrophic chondrocytes and *Vegf receptor* expression is reduced in interdigital mesenchyme. Furthermore, we showed that FGF18 was sufficient to induce *Vegf* expression in chondrocytes and the perichondrium in a limb explant culture system. The decreased *Vegf* expression in hypertrophic chondrocytes could be either a direct effect of FGF18/FGFR3 signaling or an indirect consequence of delayed terminal differentiation of hypertrophic chondrocytes. In support of this model, Amizuka et al. demonstrated that *Vegf* expression was greatly reduced in *Fgfr3*$^{-/-}$ hypertrophic chondrocytes (Amizuka et al., 2004).

Concluding remarks

Our previous studies (Liu et al., 2002) and data presented here demonstrate that FGF18 regulates chondrocyte proliferation and differentiation by signaling to FGFR3 in proliferating chondrocytes and osteogenesis by signaling to FGFR1 and/or FGFR2 in the perichondrium/periosteum. Here we present further evidence that FGF18 signaling is also important for early chondrocyte proliferation, initiation of chondrocyte hypertrophy and for vascularization of the growth plate. FGF18 thus functions to coordinate the three critical developmental stages of endochondral ossification by balancing the developmental timing of chondrogenesis, osteogenesis and vascularization.

Acknowledgments

We thank L. Li, C. Smith, and G. Schmid for their technical help. This work was supported by NIH grant HD049808, Washington University institutional funds and a gift from the Virginia Friedhofer Charitable Trust.

References

Amizuka, N., Davidson, D., Liu, H., Valverde-Franco, G., Chai, S., Maeda, T., Ozawa, H., Hammond, V., Ornitz, D.M., Goltzman, D., Henderson, J.E., 2004. Signalling by fibroblast growth factor receptor 3 and parathyroid hormone-related peptide coordinate cartilage and bone development. Bone 34, 13–25.

Barleon, B., Siemeister, G., Martiny-Baron, G., Weindel, K., Herzog, C., Marme, D., 1997. Vascular endothelial growth factor up-regulates its receptor fms-like tyrosine kinase 1 (FLT-1) and a soluble variant of FLT-1 in human vascular endothelial cells. Cancer Res. 57, 5421–5425.

Carlevaro, M.F., Cermelli, S., Cancedda, R., Descalzi Cancedda, F., 2000. Vascular endothelial growth factor (VEGF) in cartilage neovascularization and chondrocyte differentiation: auto-paracrine role during endochondral bone formation. J. Cell Sci. 113 (Pt 1), 59–69.

Chikazu, D., Hakeda, Y., Ogata, N., Nemoto, K., Itabashi, A., Takato, T., Kumegawa, M., Nakamura, K., Kawaguchi, H., 2000. Fibroblast growth factor (FGF)-2 directly stimulates mature osteoclast function through activation of FGF receptor 1 and p42/p44 MAP kinase. J. Biol. Chem. 275, 31444–31450.

Chikazu, D., Katagiri, M., Ogasawara, T., Ogata, N., Shimoaka, T., Takato, T., Nakamura, K., Kawaguchi, H., 2001. Regulation of osteoclast differentiation by fibroblast growth factor 2: stimulation of receptor activator of nuclear factor kappaB ligand/osteoclast differentiation factor expression in osteoblasts and inhibition of macrophage colony-stimulating factor function in osteoclast precursors. J. Bone Miner. Res. 16, 2074–2081.

Colvin, J.S., Bohne, B.A., Harding, G.W., McEwen, D.G., Ornitz, D.M., 1996. Skeletal overgrowth and deafness in mice lacking fibroblast growth factor receptor 3. Nat. Genet. 12, 390–397.

Cross, M.J., Claesson-Welsh, L., 2001. FGF and VEGF function in angiogenesis: signalling pathways, biological responses and therapeutic inhibition. Trends Pharmacol. Sci. 22, 201–207 (Review).

Davidson, D., Blanc, A., Filion, D., Wang, H., Plut, P., Pfeffer, G., Buschmann, M.D., Henderson, J.E., 2005. FGF18 signals through FGFR3 to promote chondrogenesis. J. Biol. Chem. 280, 20509–20515.

Erlebacher, A., Filvaroff, E.H., Gitelman, S.E., Derynck, R., 1995. Toward a molecular understanding of skeletal development. Cell 80, 371–378.

Fitzsimmons, T.J., Gukovsky, I., McRoberts, J.A., Rodriguez, E., Lai, F.A., Pandol, S.J., 2000. Multiple isoforms of the ryanodine receptor are expressed in rat pancreatic acinar cells. Biochem. J. 351, 265–271.

Gerber, H.P., Vu, T.H., Ryan, A.M., Kowalski, J., Werb, Z., Ferrara, N., 1999. VEGF couples hypertrophic cartilage remodeling, ossification and angiogenesis during endochondral bone formation. Nat. Med. 5, 623–628.

Goldring, M.B., Tsuchimochi, K., Ijiri, K., 2006. The control of chondrogenesis. J. Cell. Biochem. 97, 33–44.

Haigh, J.J., Gerber, H.P., Ferrara, N., Wagner, E.F., 2000. Conditional inactivation of VEGF-A in areas of collagen2a1 expression results in embryonic lethality in the heterozygous state. Development 127, 1445–1453.

Iwata, T., Chen, L., Li, C., Ovchinnikov, D.A., Behringer, R.R., Francomano, C.A., Deng, C.X., 2000. A neonatal lethal mutation in FGFR3 uncouples proliferation and differentiation of growth plate chondrocytes in embryos. Hum. Mol. Genet. 9, 1603–1613.

Karsenty, G., 2003. The complexities of skeletal biology. Nature 423, 316–318.

Karsenty, G., Wagner, E.F., 2002. Reaching a genetic and molecular understanding of skeletal development. Dev. Cell 2, 389–406.

Kronenberg, H.M., 2003. Developmental regulation of the growth plate. Nature 423, 332–336.

Lavine, K.J., White, A.C., Park, C., Smith, C.S., Choi, K., Long, F., Hui, C.C., Ornitz, D.M., 2006. Fibroblast growth factor signals regulate a wave of Hedgehog activation that is essential for coronary vascular development. Genes Dev. 20, 1651–1666.

Liu, Z., Xu, J., Colvin, J.S., Ornitz, D.M., 2002. Coordination of chondrogenesis and osteogenesis by fibroblast growth factor 18. Genes Dev. 16, 859–869.

Maes, C., Carmeliet, P., Moermans, K., Stockmans, I., Smets, N., Collen, D., Bouillon, R., Carmeliet, G., 2002. Impaired angiogenesis and endochondral bone formation in mice lacking the vascular endothelial growth factor isoforms VEGF164 and VEGF188. Mech. Dev. 111, 61–73.

Mills, J.C., Syder, A.J., Hong, C.V., Guruge, J.L., Raaii, F., Gordon, J.I., 2001. A molecular profile of the mouse gastric parietal cell with and without exposure to *Helicobacter pylori*. Proc. Natl. Acad. Sci. U. S. A. 98, 13687–13692.

Minina, E., Wenzel, H.M., Kreschel, C., Karp, S., Gaffield, W., McMahon, A.P., Vortkamp, A., 2001. BMP and Ihh/PTHrP signaling interact to coordinate chondrocyte proliferation and differentiation. Development 128, 4523–4534.

Miquerol, L., Gertsenstein, M., Harpal, K., Rossant, J., Nagy, A., 1999. Multiple developmental roles of VEGF suggested by a LacZ-tagged allele. Dev. Biol. 212, 307–322.

Naski, M.C., Colvin, J.S., Coffin, J.D., Ornitz, D.M., 1998. Repression of hedgehog signaling and BMP4 expression in growth plate cartilage by fibroblast growth factor receptor 3. Development 125, 4977–4988.

Naski, M.C., Wang, Q., Xu, J., Ornitz, D.M., 1996. Graded activation of fibroblast growth factor receptor 3 by mutations causing achondroplasia and thanatophoric dysplasia. Nat. Genet. 13, 233–237.

Ohbayashi, N., Shibayama, M., Kurotaki, Y., Imanishi, M., Fujimori, T., Itoh, N., Takada, S., 2002. FGF18 is required for normal cell proliferation and differentiation during osteogenesis and chondrogenesis. Genes Dev. 16, 870–879.

Ornitz, D.M., 2005. FGF signaling in the developing endochondral skeleton. Cytokine Growth Factor Rev. 16, 205–213.

Ornitz, D.M., Marie, P.J., 2002. FGF signaling pathways in endochondral and intramembranous bone development and human genetic disease. Genes Dev. 16, 1446–1465.

Roodman, G.D., 1996. Advances in bone biology: the osteoclast. Endocr. Rev. 17, 308–332.

Sahni, M., Ambrosetti, D.C., Mansukhani, A., Gertner, R., Levy, D., Basilico, C., 1999. FGF signaling inhibits chondrocyte proliferation and regulates bone development through the STAT-1 pathway. Genes Dev. 13, 1361–1366.

Sahni, M., Raz, R., Coffin, J.D., Levy, D., Basilico, C., 2001. STAT1 mediates the increased apoptosis and reduced chondrocyte proliferation in mice overexpressing FGF2. Development 128, 2119–2129.

Shen, B.Q., Lee, D.Y., Gerber, H.P., Keyt, B.A., Ferrara, N., Zioncheck, T.F., 1998. Homologous up-regulation of KDR/Flk-1 receptor expression by vascular endothelial growth factor in vitro. J. Biol. Chem. 273, 29979–29985.

Shih, S.C., Robinson, G.S., Perruzzi, C.A., Calvo, A., Desai, K., Green, J.E., Ali, I.U., Smith, L.E., Senger, D.R., 2002. Molecular profiling of angiogenesis markers. Am. J. Pathol. 161, 35–41.

Vu, T.H., Shipley, J.M., Bergers, G., Berger, J.E., Helms, J.A., Hanahan, D., Shapiro, S.D., Senior, R.M., Werb, Z., 1998. MMP-9/Gelatinase B is a key regulator of growth plate angiogenesis and apoptosis of hypertrophic chondrocytes. Cell 93, 411–422.

Wagner, E.F., Karsenty, G., 2001. Genetic control of skeletal development. Curr. Opin. Genet. Dev. 11, 527–532.

Xu, J.S., Liu, Z.H., Ornitz, D.M., 2000. Temporal and spatial gradients of Fgf8 and Fgf17 regulate proliferation and differentiation of midline cerebellar structures. Development 127, 1833–1843.

Yancopoulos, G.D., Davis, S., Gale, N.W., Rudge, J.S., Wiegand, S.J., Holash, J., 2000. Vascular-specific growth factors and blood vessel formation. Nature 407, 242–248.

Zelzer, E., Olsen, B.R., 2005. Multiple roles of vascular endothelial growth factor (VEGF) in skeletal development, growth, and repair. Curr. Top. Dev. Biol. 65, 169–187.

Zelzer, E., McLean, W., Ng, Y.S., Fukai, N., Reginato, A.M., Lovejoy, S., D'Amore, P.A., Olsen, B.R., 2002. Skeletal defects in VEGF(120/120) mice reveal multiple roles for VEGF in skeletogenesis. Development 129, 1893–1904.